


## Original Article

## DNA Methylation-Dependent Regulation of Lipoprotein Lipase Expression During Human Mesenchymal Stem Cell Differentiation into Adipocytes

Seied Rasoul Razavi Babaheidari<sup>1</sup>, Aryan Salahi-Niri<sup>2</sup>, Mohammad Hossein Mohammadi<sup>3</sup>, Mohsen Hamidpour<sup>3</sup>, Shadi Esmaeili<sup>3\*</sup> <sup>1</sup> Blood Transfusion Research Center, High Institute for Research and Education in Transfusion Medicine, Tehran, Iran.<sup>2</sup> Basic and Molecular Epidemiology of Gastrointestinal Disorders Research Center, Research Institute for Gastroenterology and Liver Diseases, Shahid Beheshti University of Medical Sciences, Tehran, Iran.<sup>3</sup> Department of Hematology and Blood Banking, School of Allied Medical Sciences, Shahid Beheshti University of Medical Sciences, Tehran, Iran.Scan and read the  
article online**Citation** Razavi Babaheidari SR, Salahi-Niri A, Mohammadi MH, Hamidpour M, Esmaeili SH. DNA Methylation-Dependent Regulation of Lipoprotein Lipase Expression During Human Mesenchymal Stem Cell Differentiation into Adipocytes. Iran J Blood Cancer. 2025 Mar 30;17(1): 20-28.

## Article info:

Received: 19 Jan 2025  
Accepted: 17 Mar 2025  
Published: 30 Mar 2025

## Keywords:

Lipoprotein lipase  
DNA methylation  
Mesenchymal stem cells  
Adipogenic differentiation  
Epigenetic regulation  
Gene expression

## Abstract

**Background:** Lipoprotein lipase (LPL) is a critical enzyme in lipid metabolism that hydrolyzes triglyceride-rich lipoproteins. While its role in mature adipose tissue is well understood, the epigenetic regulation of LPL during mesenchymal stem cell (MSC) differentiation into adipocytes remains poorly characterized. This study aimed to investigate the temporal expression pattern of LPL and its relationship with DNA methylation during adipogenic differentiation of human bone marrow-derived MSCs.**Methods:** Human bone marrow MSCs were isolated and characterized using flow cytometry for specific surface markers (CD34, CD31, CD90, and CD105). Cells were differentiated into adipocytes over 14 days and osteoblasts over 21 days using specific differentiation media. Differentiation was confirmed through Oil Red O and Alizarin Red staining respectively. LPL gene expression was analyzed using both qualitative RT-PCR and quantitative real-time PCR at day 0 (undifferentiated) and day 14 (differentiated) timepoints. DNA methylation patterns were assessed using methylation-specific PCR (MSP) following bisulfite conversion, with collagen gene serving as an internal control.**Results:** Flow cytometry confirmed MSC identity through positive expression of CD166, CD13, CD105, and CD44. Successful adipogenic differentiation was demonstrated by Oil Red O-positive lipid droplet accumulation, while osteogenic differentiation was confirmed by Alizarin Red S staining of calcium deposits. LPL gene expression was absent in undifferentiated MSCs but showed significant expression in differentiated adipocytes at day 14, coinciding with morphological changes and lipid accumulation.**Conclusion:** This study demonstrates that LPL expression is epigenetically regulated during MSC differentiation into adipocytes, with significant changes in both gene expression and DNA methylation patterns. The temporal correlation between LPL expression, methylation status, and adipogenic differentiation suggests that LPL serves as a key molecular switch in this process.

## \* Corresponding Author:

Shadi Esmaeili

**Affiliation:** Department of Hematology and Blood Banking, School of Allied Medical Sciences, Shahid Beheshti University of Medical Sciences, Tehran, Iran.**E-mail:** [sh.esmaeili@sbmu.ac.ir](mailto:sh.esmaeili@sbmu.ac.ir)

## 1. INTRODUCTION

Lipoprotein lipase (LPL) plays a central role in lipid metabolism as a key enzyme responsible for hydrolyzing triglyceride-rich lipoproteins and facilitating fatty acid uptake (1). The regulation of LPL expression and activity is crucial for maintaining lipid homeostasis, with its dysregulation being implicated in various metabolic disorders (2). While LPL's function in mature adipose tissue is well-documented, its regulation during the process of mesenchymal stem cell (MSC) differentiation into adipocytes remains incompletely understood, particularly regarding epigenetic mechanisms of control (3).

MSCs, multipotent cells capable of differentiating into various cell types including adipocytes, serve as an excellent model system for studying the molecular mechanisms underlying adipogenesis (4, 5). The differentiation of MSCs into adipocytes involves complex transcriptional programming and epigenetic modifications that orchestrate the expression of adipogenic genes (6). DNA methylation, a major epigenetic modification, has emerged as a critical regulator of gene expression during cell differentiation and development (7). Recent evidence suggests that changes in DNA methylation patterns can significantly influence the expression of genes involved in adipogenesis and lipid metabolism (8, 9).

LPL regulation during adipogenic differentiation represents a particularly interesting area of study, as this enzyme not only serves as a marker of adipocyte differentiation but also plays a functional role in lipid accumulation (10). While previous studies have established that LPL expression increases during adipogenesis, the epigenetic mechanisms controlling this upregulation, particularly the role of DNA methylation, have not been fully elucidated (11). Understanding these regulatory mechanisms is crucial, as they may provide insights into both normal adipose tissue development and pathological conditions associated with aberrant lipid metabolism (12).

In this study, we investigated the temporal expression pattern of LPL during the differentiation of human bone marrow-derived MSCs into adipocytes and examined the relationship between LPL expression and DNA methylation status. We employed a comprehensive approach combining gene expression analysis, DNA methylation profiling, and functional assessments to characterize the regulatory mechanisms controlling LPL during adipogenic differentiation. Our findings provide new insights into the epigenetic regulation of LPL and its role in adipocyte development, potentially contributing to our understanding of metabolic disorders and identifying new therapeutic targets.

## 2. MATERIALS AND METHODS

### 2.1. Ethics Statement

Ethical approval for the study was obtained from the Regional Ethics Committee of Shahid Beheshti University of Medical Sciences. Informed consent was obtained from healthy participants at Taleghani Hospital in Tehran, and bone marrow samples were collected through aspiration procedures.

### 2.2. Cell culture

The isolated mononuclear cells were suspended at a concentration of  $1 \times 10^6$  cells/ml and cultured in T75 flasks at 37°C with 5% CO<sub>2</sub>. They were maintained in DMEM supplemented with 10% FBS, with the medium changed three times per week to support optimal growth.

For passaging, the culture medium was first removed, and adherent cells were washed three times with 20 ml of PBSA buffer. Fresh medium was then added, and the cells were allowed to grow for approximately one week until they reached 60–70% confluence. At this stage, they were enzymatically detached using trypsin and subsequently subcultured into new flasks for further expansion.

### 2.3. Differentiation of MSCs into osteoblast

Bone marrow mononuclear cells (MNCs) were isolated using Ficoll-Hypaque density gradient centrifugation. Cell viability and quantity were assessed using trypan blue staining. The isolated MNCs were then resuspended to a concentration of  $1 \times 10^6$  cells/ml.

To induce osteogenic differentiation, we prepared a culture medium composed of high glucose Dulbecco's Modified Eagle Medium (DMEM) supplemented with 10% fetal bovine serum (FBS), 8–10 µmol/L dexamethasone (Sigma, USA), 3.7 g/L sodium bicarbonate, and 0.05 g/L ascorbic acid (Sigma, USA).

The cell suspension was centrifuged at 1200 rpm for 5 minutes at 25°C. After discarding the supernatant, 1 mL of the resuspended cell solution was added to each well of a 6-well culture plate containing osteogenic differentiation medium. The plates were then incubated under standard conditions.

Medium changes were performed every 3–4 days by carefully aspirating 1 mL of spent medium and replacing it with fresh osteogenic differentiation medium. A control group was maintained in parallel using standard culture medium without differentiation factors. Cell morphology was monitored regularly using an inverted microscope. After 21

days of differentiation, the cells were stained with Alizarin Red (Sigma, USA) for analysis and imaging.

#### 2.4. Osteoblast staining with Alizarin Red

To perform Alizarin Red staining, we first washed the osteoblasts with 1× phosphate-buffered saline (PBS; Kantonsapotheke Zürich, Switzerland, Cat. No. A171012). Cells were then fixed in 4% (v/v) formaldehyde solution (Sigma, USA, Cat. No. F8775) prepared in 1× PBS for 30 minutes. After two washes with deionized water (ddH<sub>2</sub>O), we stained the cells with Alizarin Red solution (0.7 g Alizarin Red S (Sigma, USA, Cat. No. A5533) dissolved in 50 ml ddH<sub>2</sub>O and adjusted to pH 4.2) for 20 minutes. Following staining, the cells were washed four times with ddH<sub>2</sub>O, air-dried, and stored in a light-protected environment until imaging.

#### 2.5. Flow cytometric validation of MSCs

Flow cytometric analysis of cell surface markers was conducted at the Research Center of Taleghani Hospital using Passage 3 cells. To characterize the cells, four antibodies (CD34, CD31, CD90, and CD10) were used, with an unstained sample serving as the negative control. After trypsinization, the cells were resuspended in 100 µL of PBS at a concentration of 10<sup>5</sup> cells. The suspension was then incubated with 3 µL of each antibody at 4°C for 30 minutes. Following incubation, the cells were washed with 500 µL of PBS and resuspended in 300 µL of PBS. Flow cytometric analysis was performed using a BD FACS Calibur flow cytometer (USA), and data was processed with Flow Software (version 7.6.1).

#### 2.6. Differentiation of MSCs into adipocytes

Adipogenic differentiation was initiated using cells at Passage 3. When the cells reached full confluence in 6-well plates, the differentiation protocol was commenced. The adipogenic induction medium comprised Dulbecco's Modified Eagle Medium (DMEM) supplemented with 10% fetal bovine serum (FBS), 100 nM dexamethasone (Sigma, USA), and 50 µg/mL indomethacin (Sigma, USA). Control wells were maintained in standard DMEM with 10% FBS. The cultures were incubated at 37°C in a 5% CO<sub>2</sub> atmosphere for 14 days, after which adipogenic differentiation was evaluated through Oil Red O staining.

#### 2.7. Adipocyte staining with Oil red O.

For Oil Red O staining, we first washed the cells twice with PBS and then fixed them in 10% formaldehyde for 45

minutes at room temperature. Following two washes with distilled water and a single wash with 50% isopropanol, the cells were stained with filtered Oil Red O solution in 60% isopropanol for 1 hour at room temperature. Subsequently, the stained cells underwent two sequential washes, first with distilled water and then with PBS. Under light microscopy, differentiated adipocytes revealed distinct red-stained lipid droplets.

#### 2.8. DNA extraction

Genomic DNA was extracted from cells at two time points: undifferentiated MSCs (UD) during week one and differentiated adipocytes (D) at the end of week two, using the Roche DNA extraction kit. DNA quality was evaluated by agarose gel electrophoresis, and concentration was measured using a NanoDrop 1000TMS spectrophotometer (OD 260 nm/OD 280 nm) (Table 1).

#### 2.9. DNA Treatment with Sodium bisulfite (SBS) and CpG Methyltransferase (M.SssI).

##### 2.9.1. DNA Bisulfite Treatment

MSP DNA preparation was initiated through bisulfite treatment. We combined 10 µL of DNA with 40 µL deionized distilled water and 5.5 µL of 2M sodium hydroxide (NaOH), then incubated the mixture at 37°C for 20 minutes. Subsequently, we sequentially added fresh solutions of 10 mM hydroquinone (30 µL) and 3 M sodium bisulfite (520 µL), and overlaid the mixture with mineral oil. The sample was then incubated for 16 hours at 50°C, after which DNA was extracted using the Roche extraction kit. Desulfonation was accomplished by adding 22 µL of 3 M NaOH and incubating at room temperature for 5 minutes. Finally, we precipitated the DNA using ammonium acetate-ethanol and resuspended the pellet in 30 µL of deionized distilled water (ddH<sub>2</sub>O).

##### 2.9.2. Methylation-Specific PCR (MSP)

We designed methylated (M) and unmethylated (U) region-specific primers using the Methprimer online software, as detailed in Table 2. The PCR reaction mixture (25 µL) comprised the following components: 10x buffer, 1.25 mM deoxynucleotide triphosphate (dNTP) mixture, 0.5 µM of each primer, 25 mM magnesium chloride (MgCl<sub>2</sub>), 1-4% dimethyl sulfoxide (DMSO), 1.25 units of Taq DNA Polymerase (Fermentas), and 50 ng of bisulfite-treated DNA. Each methylation-specific PCR (MSP) analysis was conducted in triplicate.

The primer sets for methylated (LPL-M) and unmethylated (LPL-U) regions produced amplification products of 124 base pairs (bp) and 128 bp, respectively. The methylated primers (LPLM3-F/R) exhibited melting temperature ( $T_m$ ) values of 52.2°C for the forward primer and 46.3°C for the reverse primer. Conversely, the unmethylated primers (LPLU3-F/R) demonstrated  $T_m$  values of 53.2°C (forward) and 47.5°C (reverse). Amplification products were subsequently visualized using 2% agarose gel electrophoresis.

### 2.9.3. Controls

A non-template control was used as a negative control to check for potential contamination. Positive control DNA was generated by methylating peripheral blood genomic DNA with the M.SssI enzyme (New England Biolabs). The methylation reaction consisted of 10 µL of 10X buffer, 0.5 µL of 32 mM S-adenosyl methionine, 2 µL of M.SssI enzyme, and 6 µL of genomic DNA, with the final volume adjusted to 100 µL using distilled water. The reaction mixture was then incubated at 37°C for 1.5 hours. This methylated DNA was used as a positive control for MSP, utilizing methylation-specific primers.

## 3. RESULTS

### 3.1. Morphological Characterization of MSCs

Microscopic examination of the isolated MSCs revealed characteristic fibroblast-like morphology when observed under an inverted microscope. The cells displayed typical spindle-shaped appearance with elongated cytoplasmic processes and adherent growth patterns consistent with MSC characteristics. These morphological features remained stable throughout the culture period. The identity of the isolated cells was confirmed through flow cytometric analysis at the stem cell research center. The cells demonstrated positive expression of established MSC surface markers. Expression analysis revealed the presence of CD166 (ALCAM), an adhesion molecule characteristic of MSCs, along with CD13, a membrane metalloprotease associated with stem cell properties. Additionally, the cells expressed CD105 (Endoglin), a key marker for MSC identification, as well as CD44, a cell-surface glycoprotein involved in cell-cell interactions.

### 3.2. Osteogenic Differentiation and Mineralization

MSCs cultured in osteoblastic differentiation medium demonstrated successful differentiation into osteoblast-like cells over a 21-day period. The progression of osteogenic

differentiation was confirmed through Alizarin Red S staining, which specifically binds to calcium deposits characteristic of mineralized matrix formation. By day 21 of differentiation, extensive mineralization was evident in cultures maintained in osteogenic medium. The Alizarin Red S staining revealed distinct bright red deposits throughout the culture, indicating robust calcium deposition and matrix mineralization. This pattern of mineralization is a hallmark of successful osteogenic differentiation and demonstrates the functional capacity of the differentiated cells to produce mineralized extracellular matrix, a key characteristic of mature osteoblasts. In contrast, control cultures maintained in standard growth medium showed no evidence of mineralization, appearing negative for Alizarin Red S staining. This differential staining pattern between treated and control cultures confirms that the observed mineralization was specifically induced by the osteogenic differentiation conditions and not due to spontaneous differentiation. The presence of these calcium-rich deposits, visualized through Alizarin Red S staining, provides strong evidence for the successful differentiation of MSCs into functional osteoblasts capable of producing mineralized matrix.

Also, MSCs exposed to adipogenic differentiation medium underwent successful transformation into adipocyte-like cells over a 14-day culture period. The progression of adipogenic differentiation was monitored and confirmed through Oil Red O staining, which specifically identifies intracellular lipid droplets characteristic of mature adipocytes.

By day 14 of differentiation, cells displayed significant morphological changes consistent with adipogenic conversion. The most notable change was the appearance of numerous spherical lipid droplets within the cytoplasm, a distinctive feature of adipocyte development. Oil Red O staining revealed these lipid accumulations as bright red droplets distributed throughout the differentiated cells, demonstrating successful adipogenic conversion of the MSCs.

The differentiated cells exhibited multiple lipid vacuoles of varying sizes, indicating different stages of lipid accumulation and adipocyte maturation. This heterogeneous pattern of lipid accumulation is typical of *in vitro* adipogenesis and reflects the gradual acquisition of adipocyte-specific functions. In contrast, control cultures maintained in standard growth medium retained their characteristic fibroblast-like morphology and showed no evidence of lipid accumulation when subjected to Oil Red O staining.



The presence and distribution of these Oil Red O-positive lipid droplets provides compelling evidence for the successful differentiation of MSCs into functional adipocytes capable of lipid synthesis and storage. **Figure 1.** illustrates validation of MSC multipotency through osteogenic and adipogenic differentiation.

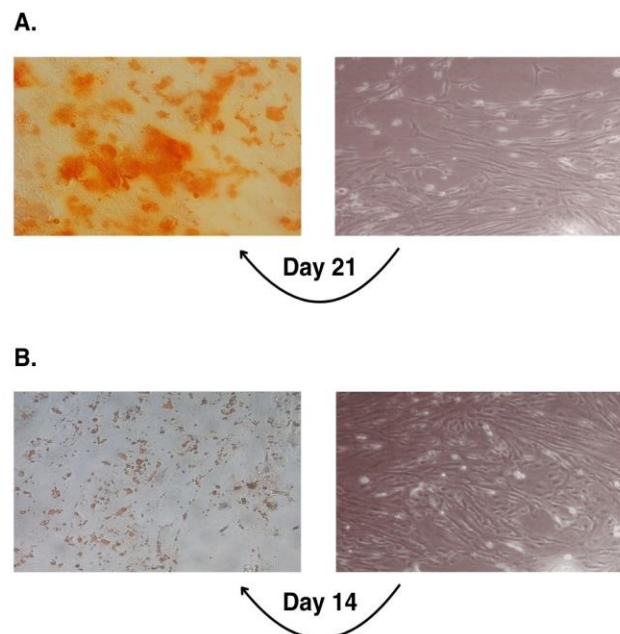


**Figure 1. A.** Osteogenic differentiation assessed by Alizarin Red S staining at day 21. Left panel: MSCs cultured in osteogenic differentiation medium showing extensive calcium deposition (bright red staining). Right panel: Control MSCs maintained in standard growth medium showing no mineralization. Magnification: 100 $\times$ .

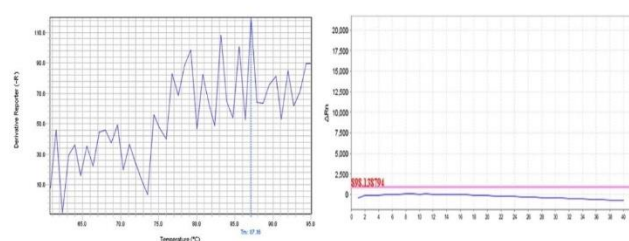
**B.** Adipogenic differentiation assessed by Oil Red O staining at day 14. Left panel: MSCs cultured in adipogenic differentiation medium showing abundant lipid droplet accumulation (bright red staining). Right panel: Control MSCs maintained in standard growth medium showing no lipid accumulation. Magnification: 100 $\times$ .

### 3.3. RT-PCR analyses conducted prior to and subsequent to the differentiation of MSCs into adipocytes

The expression pattern of the LPL gene was analyzed using qualitative RT-PCR at two critical time points: in undifferentiated MSCs (day 0) and in fully differentiated adipocytes (day 14 post-induction). This temporal analysis revealed a distinct shift in LPL expression associated with adipogenic differentiation (**Figure 2**).

In undifferentiated MSCs (day 0), LPL gene expression was notably absent, consistent with the uncommitted state of these stem cells. However, following 14 days of adipogenic induction, the differentiated cells demonstrated clear LPL expression, indicating successful activation of the adipocyte-

### A. Before differentiation



### B. After differentiation

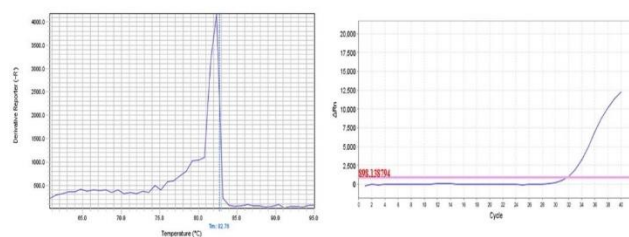


**Figure 2. A.** Analysis of undifferentiated MSCs (day 0): Representative amplification plot (left) showing PCR cycle number versus fluorescence intensity, and corresponding melting curve analysis (right) demonstrating specificity of LPL gene amplification.

**B.** Analysis of differentiated adipocytes (day 14): Representative amplification plot (left) showing PCR cycle number versus fluorescence intensity, and corresponding melting curve analysis (right) demonstrating specificity of LPL gene amplification.

specific transcriptional program. This marked induction of LPL expression coincided with the morphological changes and lipid accumulation observed during adipogenic differentiation.

The presence of LPL transcripts in differentiated cells is particularly significant as LPL is a key enzyme in lipid metabolism and serves as a well-established marker of mature adipocytes. Its expression is tightly regulated during adipogenesis and is essential for the functional capacity of mature adipocytes to process and store lipids. The observed pattern of LPL expression - from complete absence in undifferentiated MSCs to clear presence in differentiated cells - provides molecular confirmation of successful adipogenic differentiation at the transcriptional level. **Figure 2** Sets out real-time PCR analysis of LPL gene expression during MSC adipogenic differentiation.

### 3.4. Outcomes of qRT-PCR elucidate the process of adipocyte differentiation from MSCs utilizing a differentiation medium

The temporal expression profile of the LPL gene during adipogenic differentiation was quantitatively assessed using real-time quantitative RT-PCR (qRT-PCR). Samples were

analyzed at two critical time points: undifferentiated MSCs (day 0) and terminally differentiated adipocytes (day 14 post-induction), using gene-specific primers designed to detect LPL transcripts.

The qRT-PCR analysis provided precise quantification of LPL expression levels, enabling direct comparison between the undifferentiated and differentiated states. RNA was extracted from both time points, reverse transcribed to cDNA, and subjected to qRT-PCR analysis under standardized conditions. The specificity of amplification was confirmed through melting curve analysis, ensuring the accuracy of the quantitative measurements.

Gene expression was normalized to an appropriate housekeeping gene to account for potential variations in RNA input and reverse transcription efficiency. This normalization strategy allowed for reliable comparison of LPL expression levels between the two time points, providing a quantitative measure of transcriptional activation during adipogenic differentiation. **Figure 3** illustrates analysis of LPL expression and methylation status during MSC adipogenic differentiation.

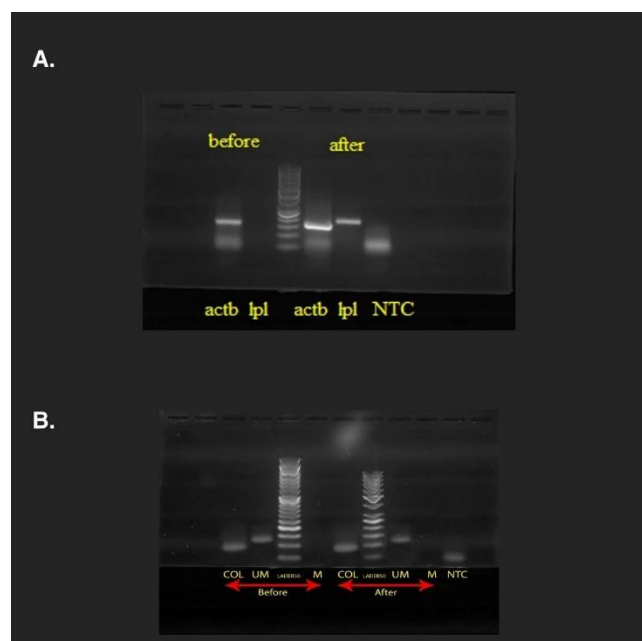


**Figure 3.** A. RT-PCR analysis of LPL expression during adipogenic differentiation. Lanes from left to right: beta-actin (pre-differentiation), LPL (pre-differentiation), 50bp DNA ladder, beta-actin (day 14 post-differentiation), LPL (day 14 post-differentiation), and no template control (NTC). Beta-actin served as internal control for normalization.

B. Methylation-specific PCR (MSP) analysis of the LPL promoter region. Lanes from left to right: collagen gene control (pre-differentiation), unmethylated-specific primer amplification (pre-differentiation), 50bp DNA ladder, methylated-specific primer amplification (pre-differentiation), collagen gene control (day 14

post-differentiation), unmethylated-specific primer amplification (day 14 post-differentiation), methylated-specific primer amplification (day 14 post-differentiation), and no template control (NTC). Collagen gene served as internal control for bisulfite conversion efficiency.

### 3.5. DNA Methylation Analysis of MSCs Before and After Adipogenic Differentiation Methylation-Specific PCR (MSP) Analysis

The methylation status of DNA was assessed in both undifferentiated MSCs and adipocyte-differentiated cells using methylation-specific PCR (MSP) following bisulfite conversion. To validate the efficiency of the bisulfite treatment, the collagen gene was used as an internal control. This gene serves as an ideal control due to its constitutively methylated status in these cell types.

The successful conversion of DNA by bisulfite treatment was confirmed by analyzing the collagen gene sequence. In its naturally methylated state, the collagen gene undergoes predictable chemical modifications during bisulfite treatment, where unmethylated cytosines are converted to uracil while methylated cytosines remain unchanged. This conversion pattern provides a reliable indicator of complete and successful bisulfite modification of the DNA samples.

## 4. DISCUSSION

This study offers comprehensive insights into the differentiation potential of MSCs and the molecular mechanisms driving adipogenic differentiation, with a particular emphasis on DNA methylation patterns and gene expression changes of the LPL gene. **Figure 4** summarizes the LPL gene methylation process.

Our investigation began with the successful isolation and characterization of MSCs from bone marrow aspirates. The isolated cells demonstrated the classical hallmarks of MSCs, including characteristic fibroblast-like morphology and adherent growth patterns. Flow cytometric analysis confirmed their identity through positive expression of established MSC markers including CD166, CD13, CD105, and CD44, validating the purity and identity of our starting cell population.

To demonstrate the multipotency of the isolated MSCs, we conducted parallel differentiation experiments along both osteogenic and adipogenic lineages. The osteogenic differentiation capacity was conclusively demonstrated over a 21-day period, with Alizarin Red S staining revealing extensive calcium deposition and matrix mineralization - hallmark characteristics of functional osteoblasts. This robust mineralization was specifically observed in cells exposed to osteogenic conditions, while control cultures

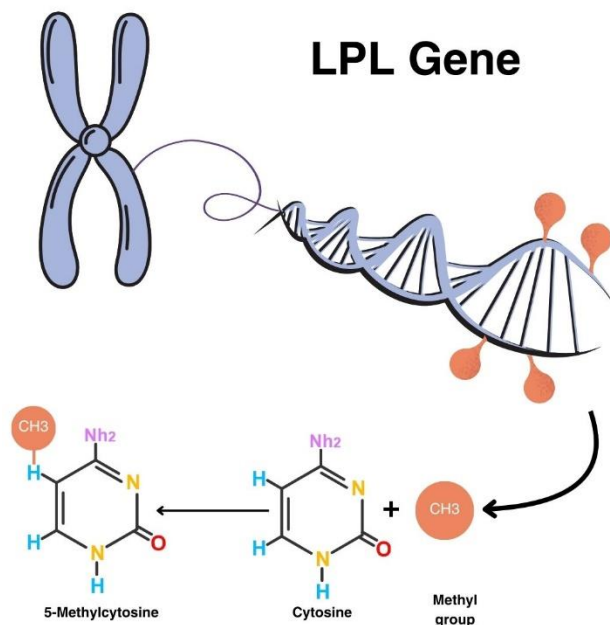


**Figure 4.** Summary of the LPL gene methylation process.

maintained in standard medium showed no evidence of spontaneous differentiation. The adipogenic differentiation potential was evaluated over a 14-day period, with successful conversion of MSCs into adipocyte-like cells confirmed through multiple complementary approaches. Morphological analysis revealed the characteristic accumulation of lipid droplets, visualized through Oil Red O staining, demonstrating the cells' acquired capacity for lipid synthesis and storage. This phenotypic transformation was accompanied by significant molecular changes, particularly in the expression of the LPL gene, a key marker of adipocyte differentiation.

Our molecular analysis revealed a striking temporal pattern in LPL expression. Qualitative RT-PCR demonstrated the absence of LPL transcripts in undifferentiated MSCs, followed by clear expression in differentiated adipocytes, indicating successful activation of the adipogenic transcriptional program. This pattern was further quantified through qRT-PCR analysis, providing precise measurements of the transcriptional changes occurring during differentiation.

To investigate the epigenetic mechanisms potentially governing these expression changes, we employed MSP following bisulfite conversion. The successful implementation of this technique was validated using the collagen gene as an internal control, ensuring the reliability of our methylation analysis. This approach allowed us to examine the relationship between DNA methylation

patterns and the observed changes in gene expression during adipogenic differentiation.

Our findings contribute to the growing body of knowledge regarding the molecular mechanisms controlling stem cell differentiation and highlight the intricate relationship between epigenetic modifications and lineage-specific gene expression (13, 14). The coordinated changes in both cellular phenotype and molecular profiles observed during differentiation underscore the complex regulatory networks governing stem cell fate decisions (15, 16).

These results have important implications for understanding the fundamental biology of stem cell differentiation and may inform future therapeutic applications in regenerative medicine. Further studies building on these findings could explore additional epigenetic modifications and their role in controlling stem cell fate, potentially leading to more efficient differentiation protocols for clinical applications.

When compared with Castellano-Castillo's 2017 work (17), there are notable parallels in how DNA methylation status influences metabolic regulation. While they focused on metabolic syndrome patients and found that LPL methylation was associated with triglyceride levels and metabolic abnormalities, our study demonstrated similar epigenetic regulation but specifically in the context of MSC differentiation. This suggests conserved regulatory mechanisms across different physiological contexts (18).

The findings from Choi et al.'s 2012 research on long-term MSC culture provide an interesting counterpoint to our work (19). Though both studies examined methylation changes in MSCs, Choi focused on senescence-related changes while our work specifically targeted differentiation-associated changes. Nevertheless, both studies highlight how cellular state transitions - whether through aging or differentiation - are accompanied by significant changes in methylation patterns that affect gene expression (20).

Our results show some notable differences when compared to Guay et al.'s 2013 findings (21). While they observed positive correlations between LPL methylation and HDL-C levels in blood cells of familial hypercholesterolemia patients, our study found decreased LPL expression during adipogenic differentiation. This apparent discrepancy likely reflects the tissue-specific nature of epigenetic regulation, with LPL potentially serving different functions in blood cells versus adipose tissue (22). Our work specifically advances the field by providing detailed analysis of how LPL methylation changes during the MSC-to-adipocyte transition, offering new insights into the temporal dynamics of this process. The combined findings from these studies, including ours, suggest that while LPL methylation

consistently plays a role in lipid metabolism, its specific patterns and effects may vary depending on cell type, physiological context, and disease state.

## 5. CONCLUSION

Based on the experimental findings and comparative analysis with previous research, this study demonstrates that LPL gene expression undergoes significant changes during the differentiation of bone marrow-derived MSCs into adipocytes, accompanied by corresponding alterations in DNA methylation patterns. We observed that LPL gene expression was notably absent in undifferentiated MSCs but showed clear expression following 14 days of adipogenic differentiation, coinciding with successful morphological transformation and lipid accumulation. This temporal pattern of LPL expression was validated through both qualitative RT-PCR and quantitative real-time PCR analyses, confirming the gene's activation during adipogenic differentiation. The methylation analysis revealed dynamic epigenetic regulation of the LPL gene during this process, with DNA methylation patterns changing as cells progressed from undifferentiated MSCs to mature adipocytes. These findings not only enhance our understanding of the molecular mechanisms governing adipogenic differentiation but also provide new insights into the epigenetic regulation of LPL in stem cell biology. The correlation between LPL expression, methylation status, and functional outcomes such as lipid accumulation suggests that LPL serves as a key molecular switch in adipogenic differentiation. This study contributes valuable knowledge to the field of stem cell biology and metabolic regulation, with potential implications for understanding adipose tissue development and metabolic disorders. Future research could further explore the precise mechanisms by which methylation changes regulate LPL expression and investigate potential therapeutic applications in metabolic diseases. Graphical abstract of the study has been provided in **Figure 5**.

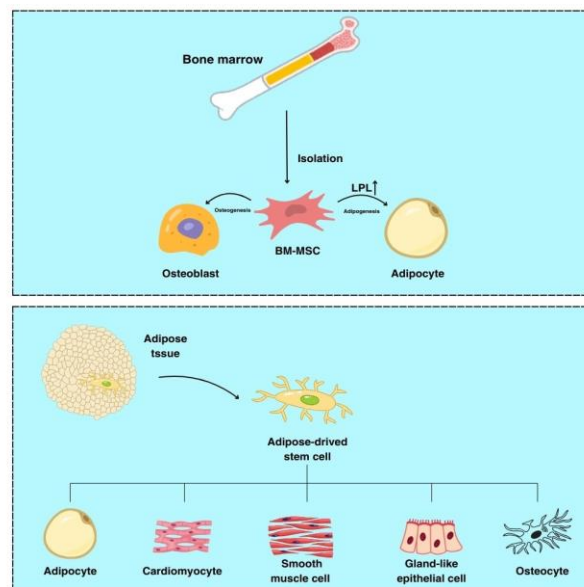


**Figure 5.** Graphical abstract of the study.

## Acknowledgment

The authors would like to express their gratitude to the reviewers and editors for their constructive feedback and suggestions, which greatly improved the quality of this manuscript.

## Conflict of interest

The authors declare that they have no conflict of interests.

## References

1. Geldenhuys WJ, Lin L, Darvesh AS, Sadana P. Emerging strategies of targeting lipoprotein lipase for metabolic and cardiovascular diseases. *Drug Discov Today*. 2017;22(2):352-65.
2. Wang H, Eckel RH. Lipoprotein lipase: from gene to obesity. *American Journal of Physiology-Endocrinology and Metabolism*. 2009;297(2):E271-E88.
3. Kockx M, Kritharides L. Triglyceride-Rich Lipoproteins. *Cardiology Clinics*. 2018;36(2):265-75.
4. Liu SS, Fang X, Wen X, Liu JS, Alip M, Sun T, et al. How mesenchymal stem cells transform into adipocytes: Overview of the current understanding of adipogenic differentiation. *World J Stem Cells*. 2024;16(3):245-56.
5. Pamplona JH, Zoehler B, Shigunov P, Barisón MJ, Severo VR, Erich NM, et al. Alternative Methods as Tools for Obesity Research: In Vitro and In Silico Approaches. *Life (Basel)*. 2022;13(1).
6. Pittenger MF, Discher DE, Péault BM, Phinney DG, Hare JM, Caplan AI. Mesenchymal stem cell perspective: cell biology to clinical progress. *npj Regenerative Medicine*. 2019;4(1):22.



7. Kolf CM, Cho E, Tuan RS. Mesenchymal stromal cells: Biology of adult mesenchymal stem cells: regulation of niche, self-renewal and differentiation. *Arthritis Research & Therapy*. 2007;9(1):204.
8. Ahmad B, Serpell CJ, Fong IL, Wong EH. Molecular Mechanisms of Adipogenesis: The Anti-adipogenic Role of AMP-Activated Protein Kinase. *Frontiers in Molecular Biosciences*. 2020;7.
9. Feng P, Pang P, Sun Z, Xie Z, Chen T, Wang S, et al. Enhancer-mediated FOXO3 expression promotes MSC adipogenic differentiation by activating autophagy. *Biochimica et Biophysica Acta (BBA) - Molecular Basis of Disease*. 2024;1870(2):166975.
10. Gonzales AM, Orlando RA. Role of adipocyte-derived lipoprotein lipase in adipocyte hypertrophy. *Nutr Metab (Lond)*. 2007;4:22.
11. Enerbäck S, Ohlsson BG, Samuelsson L, Bjursell G. Characterization of the human lipoprotein lipase (LPL) promoter: evidence of two cis-regulatory regions, LP-alpha and LP-beta, of importance for the differentiation-linked induction of the LPL gene during adipogenesis. *Mol Cell Biol*. 1992;12(10):4622-33.
12. Kuryłowicz A. Estrogens in Adipose Tissue Physiology and Obesity-Related Dysfunction. *Biomedicines* [Internet]. 2023; 11(3).
13. Lorzadeh A, Romero-Wolf M, Goel A, Jadhav U. Epigenetic Regulation of Intestinal Stem Cells and Disease: A Balancing Act of DNA and Histone Methylation. *Gastroenterology*. 2021;160(7):2267-82.
14. Fagnocchi L, Mazzoleni S, Zippo A. Integration of Signaling Pathways with the Epigenetic Machinery in the Maintenance of Stem Cells. *Stem Cells Int*. 2016;2016:8652748.
15. Li X, Jiang O, Wang S. Molecular mechanisms of cellular metabolic homeostasis in stem cells. *International Journal of Oral Science*. 2023;15(1):52.
16. Pereira B, Correia FP, Alves IA, Costa M, Gameiro M, Martins AP, et al. Epigenetic reprogramming as a key to reverse ageing and increase longevity. *Ageing Research Reviews*. 2024;95:102204.
17. Castellano-Castillo D, Moreno-Indias I, Fernández-García JC, Alcaide-Torres J, Moreno-Santos I, Ocaña L, et al. Adipose Tissue LPL Methylation is Associated with Triglyceride Concentrations in the Metabolic Syndrome. *Clin Chem*. 2018;64(1):210-8.
18. Heindel JJ, Blumberg B, Cave M, Machtinger R, Mantovani A, Mendez MA, et al. Metabolism disrupting chemicals and metabolic disorders. *Reproductive Toxicology*. 2017;68:3-33.
19. Choi MR, In Y-H, Park J, Park T, Jung KH, Chai JC, et al. Genome-scale DNA methylation pattern profiling of human bone marrow mesenchymal stem cells in long-term culture. *Experimental & Molecular Medicine*. 2012;44(8):503-12.
20. Chinn CA, Ren H, Morival JLP, Nie Q, Wood MA, Downing TL. Examining age-dependent DNA methylation patterns and gene expression in the male and female mouse hippocampus. *Neurobiol Aging*. 2021;108:223-35.
21. Guay SP, Brisson D, Lamarche B, Marceau P, Vohl MC, Gaudet D, et al. DNA methylation variations at CETP and LPL gene promoter loci: new molecular biomarkers associated with blood lipid profile variability. *Atherosclerosis*. 2013;228(2):413-20.
22. Shi Y, Zhang H, Huang S, Yin L, Wang F, Luo P, et al. Epigenetic regulation in cardiovascular disease: mechanisms and advances in clinical trials. *Signal Transduction and Targeted Therapy*. 2022;7(1):200.